

# High-accuracy numerical methods and convergence analysis for Schrödinger equation with incommensurate potentials

Kai Jiang<sup>1</sup>, Shifeng Li<sup>1</sup>, Juan Zhang<sup>1</sup>

<sup>1</sup>Department of Mathematics and Computational Science, Xiangtan University, Xiangtan, Hunan, 411105, P. R. China.

Contributing authors: [kaijiang@xtu.edu.cn](mailto:kaijiang@xtu.edu.cn); [shifengli@smail.xtu.edu.cn](mailto:shifengli@smail.xtu.edu.cn); [zhangjuan@xtu.edu.cn](mailto:zhangjuan@xtu.edu.cn);

## Abstract

Numerical solving the Schrödinger equation with incommensurate potentials presents a great challenge since its solutions could be space-filling quasiperiodic structures without translational symmetry nor decay. In this paper, we propose two high-accuracy numerical methods to solve the time-dependent quasiperiodic Schrödinger equation. Concretely, we discretize the spatial variables by the quasiperiodic spectral method and the projection method, and the time variable by the second-order operator splitting method. The corresponding convergence analysis is also presented and shows that the proposed methods both have exponential convergence rate in space and second order accuracy in time, respectively. Meanwhile, we analyse the computational complexity of these numerical algorithms. One- and two-dimensional numerical results verify these convergence conclusions, and demonstrate that the projection method is more efficient.

**Keywords:** Quasiperiodic Schrödinger equation, Quasiperiodic spectral method, Projection method, Second-order operator splitting method, Convergence analysis.

## 1 Introduction

In this paper, we consider the time-dependent quasiperiodic Schrödinger equation (TQSE)

$$i \frac{\partial u(\mathbf{x}, t)}{\partial t} = -\Delta u(\mathbf{x}, t) + V(\mathbf{x})u(\mathbf{x}, t) + f(\mathbf{x}, t), \quad (\mathbf{x}, t) \in \mathbb{R}^d \times [0, T], \quad (1)$$

where  $\Delta = \partial_{x_1}^2 + \cdots + \partial_{x_d}^2$  is the Laplacian operator,  $V(\mathbf{x})$  is the incommensurate potential,  $f(\mathbf{x}, t)$  is an external field function and  $u(\mathbf{x}, t)$  is quasiperiodic in  $\mathbf{x}$ . The initial value  $u(\mathbf{x}, 0) = u_0(\mathbf{x})$ .

The Schrödinger equation is a fundamental equation in quantum mechanics. The study of the Schrödinger equation with periodic potentials has reached a relatively mature stage [1, 2]. In the last few decades, the (nonlinear) quasiperiodic Schrödinger equations (QSEs) and quasiperiodic Schrödinger operators, have been attracted much attention due to the fascinating phenomena such as Anderson localization, mobility edge, topological phase transition [3–9]. Many mathematical works have been presented to study these incommensurate systems. Kuksin and Pöschel’s earlier work established the existence of quasiperiodic solutions in time direction for one-dimensional nonlinear QSEs by extending the Kolmogorov-Arnold-Moser (KAM) method to infinite dimensions [12]. Bourgain developed the modified Craig-Wayne method to prove the existence of quasiperiodic solutions for nonlinear QSE with periodic or spatial Dirichlet boundary conditions [14, 15]. A recent work by Berti and Bolle investigated the existence of time-quasiperiodic solutions of  $\mathbb{T}^d$ -QSE in  $C^\infty$ -space by the Nash-Moser iteration [17, 18]. Besides, Cong *et al.* studied Anderson localization of the nonlinear time-quasiperiodic Schrödinger equation by using the Birkhoff normal form transform [16]. While the time-quasiperiodic Schrödinger equation has received considerable attention, there are few theoretical results available for the spatial quasiperiodic Schrödinger equation. Recently, Wang has constructed spatial quasiperiodic solutions to the nonlinear Schrödinger equation (NLS) on  $\mathbb{R}^d$  [19]. Furthermore, the time-space quasiperiodic solutions for the non-integrable NLS on  $\mathbb{R}$  have been analyzed in [20]. For the spectral theory of quasiperiodic Schrödinger operators, one can refer to [21, 22].

However, numerically solving the QSE is still a great challenge since their solutions could be quasiperiodic, globally ordered structure without translational symmetry nor decay. The periodic approximation method (PAM) has been used to obtain an approximate periodic solution within a finite domain [6]. Besides, the PAM is also used to solve and analyze the eigenvalues of Schrödinger operators [23, 24]. However, the PAM is often unsatisfactory in terms of algorithm accuracy and convergence rate, see [25] for details. Therefore, there is still a lack of highly precise and efficient numerical algorithms for solving TQSE to obtain the quasiperiodic solution, especially for the case of arbitrary dimensions. Recently, two effective numerical methods, quasiperiodic spectral method (QSM) and projection method (PM), have been proposed to solve quasiperiodic systems [26, 27]. The corresponding function approximation rate analysis of QSM and PM has been given in [28], respectively. The PM has been also applied to quasiperiodic Schrödinger eigenvalue systems [29]. Extensive studies have demonstrated that the PM can achieve high accuracy in computing various quasiperiodic systems [30–34]. However, the corresponding numerical analysis is lacking. These theoretical results and applications illuminate our problems. The purpose of this paper is to study how to efficiently solve the spatially quasiperiodic solutions of higher-dimensional quasiperiodic Schrödinger equation to high accuracy, and to establish the corresponding convergence analysis. Concretely, we apply QSM and PM to solve the quasiperiodic solution of TQSE (1) and analyze their computational complexity. Meanwhile, a rigorous error analysis shows that both algorithms have exponential convergence rates. One- and two-dimensional numerical examples are given to verify

the effectiveness of the proposed algorithms. Furthermore, we can obtain quasiperiodic solutions and show that the PM is an efficient and high-precision algorithm for solving the TQSE.

The rest of the paper is organized as follows. Section 2 proposes two methods, the PM and the QSM, coupled with the second-order operator splitting scheme, to solve TQSE (1). We also give their numerical implementation and computational complexity analysis. Section 3 introduces quasiperiodic Hilbert spaces and gives the convergence analysis of the proposed methods. Section 4 presents numerical results to further validate the theoretical analysis. Finally, the conclusion of this paper is given in Section 5.

## 2 Numerical methods

Throughout, we make use of the following notations. Let  $\Omega_L = [-L, L]^d \subset \mathbb{R}^d$  and  $|\Omega_L| = (2L)^d$ . For any vector  $\mathbf{x} \in \mathbb{R}^d$ , we define  $\|\mathbf{x}\|^2 = \sum_{j=1}^d |x_j|^2$  and  $|\mathbf{x}| = \sum_{j=1}^d |x_j|$ . For any multi-index  $\mu = (\mu_1, \dots, \mu_d) \in \mathbb{N}^d$  and  $\mathbf{x} \in \mathbb{R}^d$ , let  $\partial_{\mathbf{x}}^{\mu} = \partial_{x_1}^{\mu_1} \cdots \partial_{x_d}^{\mu_d}$ . We present the definition of the quasiperiodic function.

**Definition 2.1.** A matrix  $\mathbf{P} \in \mathbb{R}^{d \times n}$  is the projection matrix, if it belongs to the set  $\mathbb{P}^{d \times n} := \{\mathbf{P} = (\mathbf{p}_1, \dots, \mathbf{p}_n) \in \mathbb{R}^{d \times n} : \mathbf{p}_1, \dots, \mathbf{p}_n \text{ are } \mathbb{Q}\text{-linearly independent}\}$ .

**Definition 2.2.** A  $d$ -dimensional function  $u(\mathbf{x})$  is quasiperiodic if there exists an  $n$ -dimensional periodic function  $u_p$  and a projection matrix  $\mathbf{P} \in \mathbb{P}^{d \times n}$ , such that  $u(\mathbf{x}) = u_p(\mathbf{P}^T \mathbf{x})$  for all  $\mathbf{x} \in \mathbb{R}^d$ .

In particular, when  $n = d$  and  $\mathbf{p}_1, \mathbf{p}_2, \dots, \mathbf{p}_d$  form a basis of  $\mathbb{R}^d$ ,  $u(\mathbf{x})$  is periodic. For convenience, we refer to  $u_p$  in Definition 2.2 as the parent function of  $u$ . The continuous Fourier-Bohr transformation of  $u(\mathbf{x})$  is

$$\hat{u}_{\boldsymbol{\lambda}} = \lim_{L \rightarrow \infty} \frac{1}{|\Omega_L|} \int_{\Omega_L} u(\mathbf{x}) e^{-i\boldsymbol{\lambda} \cdot \mathbf{x}} d\mathbf{x} := \int u(\mathbf{x}) e^{-i\boldsymbol{\lambda} \cdot \mathbf{x}} d\mathbf{x}, \quad (2)$$

where  $\boldsymbol{\lambda} \in \mathbb{R}^d$ . The Fourier series associated to  $u(\mathbf{x})$  is

$$u(\mathbf{x}) \sim \sum_{j=1}^{\infty} \hat{u}_{\boldsymbol{\lambda}_j} e^{i\boldsymbol{\lambda}_j \cdot \mathbf{x}}, \quad (3)$$

where  $\boldsymbol{\lambda}_j \in \sigma(u) = \{\boldsymbol{\lambda} : \boldsymbol{\lambda} = \mathbf{P}\mathbf{k}, \mathbf{k} \in \mathbb{Z}^n\}$  are Fourier exponents,  $\hat{u}_{\boldsymbol{\lambda}_j}$  computed by (2) are Fourier coefficients. If the Fourier series (3) is absolutely convergent, it is also uniformly convergent. Therefore, when  $\sum_{j=1}^{\infty} |\hat{u}_{\boldsymbol{\lambda}_j}| < +\infty$ , we have

$$u(\mathbf{x}) = \sum_{j=1}^{\infty} \hat{u}_{\boldsymbol{\lambda}_j} e^{i\boldsymbol{\lambda}_j \cdot \mathbf{x}}.$$

Moreover, the Parseval equality

$$\sum_{j=1}^{\infty} |\hat{u}_{\boldsymbol{\lambda}_j}|^2 = \int |u(\mathbf{x})|^2 d\mathbf{x} \quad (4)$$

is true.

For simplicity, we consider the homogeneous TQSE, *i.e.*,  $f = 0$ , in the following analysis. For inhomogeneous  $f \neq 0$ , the presented analysis below can be easily extended. Denote the operator  $A = -\Delta$  and for a given quasiperiodic potential

$$V(\mathbf{x}) = \sum_{\lambda \in \sigma(V)} \hat{V}_\lambda e^{i\lambda \cdot \mathbf{x}}, \quad (5)$$

TQSE (1) becomes

$$\frac{\partial u}{\partial t} = -iAu - iVu. \quad (6)$$

The formal solution of (6) is

$$u(\mathbf{x}, t) = e^{-it(A+V)}u_0 = \mathcal{T}u_0, \quad (\mathbf{x}, t) \in \mathbb{R}^d \times [0, T].$$

Next, we employ QSM and PM to discretize TQSE (6) in space direction, and the second-order operator splitting (OS2) method in time direction.

## 2.1 Spatial discretization

We first introduce the QSM and the PM, respectively. For a positive integer  $N \in \mathbb{N}_0 = \mathbb{N} \setminus \{0\}$  and the given projection matrix  $\mathbf{P} \in \mathbb{P}^{d \times n}$ , denote

$$\mathbf{K}_N^n = \{\mathbf{k} = (k_j)_{j=1}^n \in \mathbb{Z}^n : -N \leq k_j < N\},$$

and  $\sigma_N = \{\lambda = \mathbf{P}\mathbf{k} : \mathbf{k} \in \mathbf{K}_N^n\}$ . The order of set  $\sigma_N$  is  $\#(\sigma_N) = (2N)^n := D$ .

### 2.1.1 QSM method

The QSM approximates the quasiperiodic function  $u(\mathbf{x})$  by the truncation operator  $\mathcal{P}_N$ , *i.e.*,

$$u(\mathbf{x}) \approx \mathcal{P}_N u(\mathbf{x}) = \sum_{\lambda_j \in \sigma_N} \hat{u}_{\lambda_j} e^{i\lambda_j \cdot \mathbf{x}}, \quad \mathbf{x} \in \mathbb{R}^d,$$

where  $\hat{u}_{\lambda_j}$  is obtained by the continuous Fourier-Bohr transformation of  $u(\mathbf{x})$ . The function approximation theory of QSM can be found in [28].

### 2.1.2 PM method

An alternative way is PM, seizing the fact that the quasiperiodic system is defined on the irrational manifold of higher-dimensional torus. Concretely, the PM efficiently computes the Fourier coefficient of the periodic parent function on a higher-dimensional torus in a pseudo-spectral manner. Then, the quasiperiodic structure can be obtained by projecting the high-dimensional periodic structure onto a corresponding irrational manifold. Let  $\mathbb{T}^n = (\mathbb{R}/2\pi\mathbb{Z})^n$  be the  $n$ -dimensional torus. To discretize  $\mathbb{T}^n$ , we

consider a fundamental domain  $[0, 2\pi)^n$  and assume that the discrete node along each dimension is the same, *i.e.*,  $N \in \mathbb{N}_0$ . Then  $[0, 2\pi)^n$  is discretized by grid points  $\mathbf{y}_j = (y_{1,j_1}, y_{2,j_2}, \dots, y_{n,j_n})$ , where  $y_{1,j_1} = j_1 h$ ,  $y_{2,j_2} = j_2 h$ ,  $\dots$ ,  $y_{n,j_n} = j_n h$ ,  $0 \leq j_1, j_2, \dots, j_n < 2N$ , with the spatial discretization size  $h = \pi/N$ . The discrete  $n$ -dimensional torus  $\mathbb{T}_N^n$  can be obtained by periodic extending these grid points  $\mathbf{y}_j$ . The grid periodic function space defined on  $\mathbb{T}_N^n$  is

$$\mathcal{G}_N := \{U : \mathbb{Z}^n \mapsto \mathbb{C} : U \text{ is } \mathbb{T}_N^n\text{-periodic}\}.$$

Given any periodic grid functions  $U_1, U_2 \in \mathcal{G}_N$ , the  $\ell^2$ -inner product is

$$\langle U_1, U_2 \rangle_N = \frac{1}{(4\pi N)^n} \sum_{\mathbf{y}_j \in \mathbb{T}_N^n} U_1(\mathbf{y}_j) \overline{U_2(\mathbf{y}_j)}. \quad (7)$$

For  $\mathbf{k}, \ell \in \mathbb{Z}^n$ , we have the discretize orthogonality

$$\langle e^{i\mathbf{k} \cdot \mathbf{y}_j}, e^{i\ell \cdot \mathbf{y}_j} \rangle_N = \begin{cases} 1, & \mathbf{k} = \ell + 2N\mathbf{m}, \mathbf{m} \in \mathbb{Z}^n, \\ 0, & \text{otherwise.} \end{cases} \quad (8)$$

The discrete Fourier coefficient of  $U \in \mathcal{G}_N$  is

$$\tilde{U}_{\mathbf{k}} = \langle U, e^{i\mathbf{k} \cdot \mathbf{y}_j} \rangle_N, \quad \mathbf{k} \in \mathbf{K}_N^n. \quad (9)$$

The PM designates  $\tilde{U}_{\mathbf{k}}$  as the Fourier-Bohr coefficient  $\tilde{u}_{\boldsymbol{\lambda}}$ ,  $\boldsymbol{\lambda} = \mathbf{P}\mathbf{k}$ . Then we obtain the discrete Fourier-Bohr expansion of  $u(\mathbf{x})$  is

$$u(\mathbf{x}_j) = \sum_{\boldsymbol{\lambda} \in \sigma_N} \tilde{u}_{\boldsymbol{\lambda}} e^{i\boldsymbol{\lambda} \cdot \mathbf{x}_j},$$

where collocation points  $\mathbf{x}_j \in \mathbb{Q}_N = \{\mathbf{x}_j = \mathbf{P}\mathbf{y}_j, \mathbf{y}_j \in \mathbb{T}_N^n\}$ . The trigonometric interpolation of  $u$  is

$$I_N u(\mathbf{x}) = \sum_{\boldsymbol{\lambda} \in \sigma_N} \tilde{u}_{\boldsymbol{\lambda}} e^{i\boldsymbol{\lambda} \cdot \mathbf{x}}. \quad (10)$$

Consequently, let  $I_N u(\mathbf{x}_j) \approx u(\mathbf{x}_j)$ . Recent function approximation theory has shown that the PM has exponential convergence [28]. From the implementation, it is apparent that the PM can use the  $n$ -dimensional fast Fourier transform (FFT) to obtain Fourier coefficients but the QSM could not.

## 2.2 Second-order operator splitting (OS2) method

The OS2 scheme is one of the most popular numerical methods of solving Schrödinger equations [35]. The basic idea of OS2 method is splitting TQSE (6) into two subproblems

$$\frac{\partial u}{\partial t} = -iAu, \quad \frac{\partial u}{\partial t} = -iVu. \quad (11)$$

For the time grid points  $0 = t_0 < t_1 < \dots < t_M = T$ , where  $t_m = m\tau$ ,  $m = 0, 1, \dots, M$ , and the time step size  $\tau = T/M$ , the OS2 method numerically approximates the solution by the recurrence relation

$$u^m = e^{-\frac{i}{2}\tau A} e^{-i\tau V} e^{-\frac{i}{2}\tau A} u^{m-1} = \mathcal{S}^m u^0 \approx u(\cdot, t_m), \quad 1 \leq m \leq M, \quad (12)$$

where  $\mathcal{S} = e^{-\frac{i}{2}\tau A} e^{-i\tau V} e^{-\frac{i}{2}\tau A}$  and  $u^0 = u(\cdot, 0)$ .

### 2.3 Numerical implementation

In numerical implementation, the semi-discrete subproblems of (11) can be solved by QSM and PM, in terms of QSM-OS2 and PM-OS2, respectively. The detailed implementation to solve TQSE (6) and computational complexity analysis are shown below.

#### 2.3.1 QSM-OS2 method

From  $t_m$  to  $t_{m+1}$ , the QSM-OS2 involves three steps.

• **QSM-OS2-Step 1.** For  $t \in [t_m, t_m + \tau/2]$ , consider the ordinary differential equation

$$\frac{\partial u}{\partial t} = -iAu, \quad (13)$$

with initial value  $u(\cdot, t_m)$ . Therefore, we have

$$\begin{aligned} u(\mathbf{x}, t_m + \frac{\tau}{2}) &\approx \phi(\mathbf{x}, t_m) = e^{-\frac{i}{2}\tau \hat{A}_N} u(\mathbf{x}, t_m) \\ &= e^{-\frac{i}{2}\tau A} \mathcal{P}_N u(\mathbf{x}, t_m) = \sum_{\lambda \in \sigma_N(u)} \hat{u}_\lambda(t_m) e^{-\frac{i}{2}\tau \|\lambda\|^2} e^{i\lambda \cdot \mathbf{x}}. \end{aligned}$$

Denote  $\hat{\phi}_\lambda(t_m) = \hat{u}_\lambda(t_m) e^{-\frac{i}{2}\tau \|\lambda\|^2}$ .

• **QSM-OS2-Step 2.** For  $t \in [t_m, t_{m+1}]$ , consider the ordinary differential equation

$$\frac{\partial u}{\partial t} = -iVu,$$

with initial value  $\phi(\mathbf{x}, t_m)$ . From the definition of  $V$  in (5), we have

$$\psi(\mathbf{x}, t_m) = \phi(\mathbf{x}, t_{m+1}) = e^{-i\tau \hat{V}_N} \phi(\mathbf{x}, t_m) = e^{-i\tau V} \mathcal{P}_N \phi(\mathbf{x}, t_m),$$

where Fourier coefficient vector  $\hat{\Psi}(t_m) = (\hat{\psi}_{\lambda_1}(t_m), \hat{\psi}_{\lambda_2}(t_m), \dots, \hat{\psi}_{\lambda_D}(t_m))$  satisfies

$$\hat{\Psi}(t_m) = e^{-i\tau \mathcal{V}} \hat{\Phi}(t_m) \quad (14)$$

with

$$\mathcal{V} = \begin{pmatrix} \hat{V}_{\lambda_1 - \lambda_1} & \hat{V}_{\lambda_1 - \lambda_2} & \cdots & \hat{V}_{\lambda_1 - \lambda_D} \\ \hat{V}_{\lambda_2 - \lambda_1} & \hat{V}_{\lambda_2 - \lambda_2} & \cdots & \hat{V}_{\lambda_2 - \lambda_D} \\ \vdots & \vdots & & \vdots \\ \hat{V}_{\lambda_D - \lambda_1} & \hat{V}_{\lambda_D - \lambda_2} & \cdots & \hat{V}_{\lambda_D - \lambda_D} \end{pmatrix},$$

and  $\hat{\Phi}(t_m) = (\hat{\phi}_{\lambda_1}(t_m), \hat{\phi}_{\lambda_2}(t_m), \dots, \hat{\phi}_{\lambda_D}(t_m))$ . Note that  $\hat{V}_{\lambda_j - \lambda_\ell}$  means the Fourier coefficient of  $V$  on the Fourier exponent  $\lambda = \lambda_j - \lambda_\ell$ .

• **QSM-OS2-Step 3.** For  $t \in [t_m, t_m + \tau/2]$ , we still consider (13) but with initial value  $\psi(\mathbf{x}, t_m)$ , and have

$$u(\mathbf{x}, t_{m+1}) \approx e^{-\frac{i}{2}\tau\tilde{A}_N} \psi(\mathbf{x}, t_m).$$

Consequently, the fully discrete scheme of QSM-OS2 can be written as

$$u_N^{m+1} = e^{-\frac{i}{2}\tau\tilde{A}_N} e^{-i\tau\tilde{V}_N} e^{-\frac{i}{2}\tau\tilde{A}_N} u_N^m = \tilde{\mathcal{S}}_N^{m+1} u^0 \approx u(\cdot, t_{m+1}), \quad 0 \leq m \leq M-1, \quad (15)$$

where

$$\tilde{\mathcal{S}}_N = e^{-\frac{i}{2}\tau\tilde{A}_N} e^{-i\tau\tilde{V}_N} e^{-\frac{i}{2}\tau\tilde{A}_N} = e^{-\frac{i}{2}\tau A} \mathcal{P}_N e^{-i\tau V} \mathcal{P}_N e^{-\frac{i}{2}\tau A} \mathcal{P}_N.$$

Note that the identity  $\mathcal{P}_N e^{-\frac{i}{2}\tau A} \mathcal{P}_N u = e^{-\frac{i}{2}\tau A} \mathcal{P}_N u$  holds.

### 2.3.2 PM-OS2 method

From  $t_m$  to  $t_{m+1}$ , the PM-OS2 contains three steps.

• **PM-OS2-Step 1.** For  $t \in [t_m, t_m + \tau/2]$ , similar to QSM-OS2-Step 1, we have

$$u(\mathbf{x}, t_m + \tau/2) \approx \phi(\mathbf{x}, t_m) = e^{-\frac{i}{2}\tau A_N} u(\mathbf{x}, t_m) = \sum_{\lambda \in \sigma_N(u)} \tilde{u}_\lambda(t_m) e^{-\frac{i}{2}\tau \|\lambda\|^2} e^{i\lambda \cdot \mathbf{x}}.$$

Then, denote  $\tilde{\phi}_\mathbf{k}(t_m) = \tilde{u}_\lambda(t_m) e^{-\frac{i}{2}\tau \|\lambda\|^2}$  with  $\lambda = P\mathbf{k}$ .

• **PM-OS2-Step 2.** Applying FFT yields

$$I_N \phi_p(\mathbf{y}_j, t_m) = \sum_{\mathbf{k} \in K_N^n} \tilde{\phi}_\mathbf{k}(t_m) e^{i\mathbf{k} \cdot \mathbf{y}_j},$$

where the grid points  $\mathbf{y}_j \in \mathbb{T}_N^n$ . For  $t \in [t_m, t_{m+1}]$ , we have

$$\psi_p(\mathbf{y}, t_m) = e^{-i\tau V_p} I_N \phi_p(\mathbf{y}, t_m),$$

where  $V_p$  is the parent function of  $V$ . Using FFT again, we have  $\tilde{\psi}_\lambda(t_m) = \langle \psi_p(\mathbf{y}_j, t_m), e^{i\mathbf{k} \cdot \mathbf{y}_j} \rangle_N$  with  $\lambda = P\mathbf{k}$ . Consequently, we can obtain

$$\psi(\mathbf{x}, t_m) = e^{-i\tau V_N} \phi(\mathbf{x}, t_m) = e^{-i\tau V} I_N \phi(\mathbf{x}, t_m).$$

• **PM-OS2-Step 3.** For  $t \in [t_m, t_m + \tau/2]$ , similar to PM-OS2-Step 1, we have

$$u(\mathbf{x}, t_{m+1}) \approx u_N^{m+1} = e^{-\frac{i}{2}\tau A_N} \psi(\mathbf{x}, t_m) = \sum_{\boldsymbol{\lambda} \in \sigma_N(u)} \tilde{\psi}_{\boldsymbol{\lambda}}(t_m) e^{-\frac{i}{2}\tau \|\boldsymbol{\lambda}\|^2} e^{i\boldsymbol{\lambda} \cdot \mathbf{x}}.$$

Therefore, we can write the fully discrete scheme of PM-OS2 as

$$u_N^{m+1} = e^{-\frac{i}{2}\tau A_N} e^{-i\tau V_N} e^{-\frac{i}{2}\tau A_N} u_N^m = \mathcal{S}_N^{m+1} u^0 \approx u(\cdot, t_{m+1}), \quad 0 \leq m \leq M-1, \quad (16)$$

where

$$\mathcal{S}_N = e^{-\frac{i}{2}\tau A_N} e^{-i\tau V_N} e^{-\frac{i}{2}\tau A_N} = e^{-\frac{i}{2}\tau A} I_N e^{-i\tau V} I_N e^{-\frac{i}{2}\tau A} I_N.$$

### 2.3.3 Computational complexity analysis

Here we analyze the computational complexity of each time step for QSM-OS2 and PM-OS2, respectively. In the implementation of QSM-OS2-Step 1 and 3, the QSM requires  $D$  multiplication operators to solve (13). In QSM-OS2-Step 2, we compute the finite terms of the Taylor expansion for  $e^{-i\tau \mathcal{V}}$ , *i.e.*,

$$e^{-i\tau \mathcal{V}} \approx \sum_{j=0}^k \frac{(-i\tau \mathcal{V})^j}{j!}. \quad (17)$$

Therefore, there require  $2(k-1)D^3 + D^2$  operators to compute (17) and  $2D^2 - D$  operators to compute (14). The computational complexity of QSM-OS2 in solving TQSE (6) is  $O(D^3)$ .

In the implementation of PM-OS2, there require  $D$  multiplication operators in PM-OS2-Step 1 and 3. However, in PM-OS2-Step 2, the availability of FFT allows us to compute the convolutions economically in physical space as dot product, only requiring  $O(D \log D)$  operators. Therefore, the computational complexity of PM-OS2 in solving TQSE (6) is  $O(D \log D)$ .

## 3 Theoretical analysis

In this section, we present the convergence analysis of QSM-OS2 and PM-OS2.

### 3.1 Preliminaries

In this subsection, we will introduce some Hilbert spaces on  $\mathbb{T}^n$  and quasiperiodic Hilbert spaces on  $\mathbb{R}^n$ .

- $L^2(\mathbb{T}^n)$  **space:**  $L^2(\mathbb{T}^n) = \left\{ U(\mathbf{y}) : \frac{1}{|\mathbb{T}^n|} \int_{\mathbb{T}^n} |U|^2 d\mathbf{y} < +\infty \right\}$ , equipped with inner product

$$(U_1, U_2)_{L^2(\mathbb{T}^n)} = \frac{1}{|\mathbb{T}^n|} \int_{\mathbb{T}^n} U_1 \bar{U}_2 d\mathbf{y}.$$



- $H^\alpha(\mathbb{T}^n)$  **space:** for any integer  $\alpha \geq 0$ , the  $\alpha$ -derivative Hilbert space on  $\mathbb{T}^n$  is

$$H^\alpha(\mathbb{T}^n) = \{U \in L^2(\mathbb{T}^n) : \|U\|_\alpha < +\infty\},$$

where  $\|U\|_\alpha = \left( \sum_{\mathbf{k} \in \mathbb{Z}^n} (1 + |\mathbf{k}|^2)^\alpha |\hat{U}_{\mathbf{k}}|^2 \right)^{1/2}$ ,  $\hat{U}_{\mathbf{k}} = (U, e^{i\mathbf{k} \cdot \mathbf{y}})_{L^2(\mathbb{T}^n)}$ . The semi-norm of  $H^\alpha(\mathbb{T}^n)$  can be defined as  $|U|_\alpha = \left( \sum_{\mathbf{k} \in \mathbb{Z}^n} |\mathbf{k}|^{2\alpha} |\hat{U}_{\mathbf{k}}|^2 \right)^{1/2}$ .

- $X_\alpha$  **space:** for any  $U \in L^2(\mathbb{T}^n)$  and  $\alpha \in \mathbb{R}$ , the Fourier series expansion is

$$U(\mathbf{y}) = \sum_{\mathbf{k} \in \mathbb{Z}^n} \hat{U}_{\mathbf{k}} e^{i\mathbf{k} \cdot \mathbf{y}},$$

the linear operator  $(-\Delta)^\alpha$  is given by

$$(-\Delta)^\alpha U = \sum_{\mathbf{k} \in \mathbb{Z}^n} \|\mathbf{k}\|^{2\alpha} \hat{U}_{\mathbf{k}} e^{i\mathbf{k} \cdot \mathbf{y}},$$

and

$$X_\alpha = \left\{ U(\mathbf{y}) = \sum_{\mathbf{k} \in \mathbb{Z}^n} \hat{U}_{\mathbf{k}} e^{i\mathbf{k} \cdot \mathbf{y}} \in L^2(\mathbb{T}^n) : \|(-\Delta)^\alpha U\|^2 = \sum_{\mathbf{k} \in \mathbb{Z}^n} |\hat{U}_{\mathbf{k}}|^2 \cdot \|\mathbf{k}\|^{4\alpha} < \infty \right\}.$$

The set  $X_\alpha$  forms a Hilbert space with inner product

$$(U, W)_{X_\alpha} = (U, W)_{L^2(\mathbb{T}^n)} + ((-\Delta)^\alpha U, (-\Delta)^\alpha W)_{L^2(\mathbb{T}^n)},$$

and

$$\|U\|_{X_\alpha}^2 = \sum_{\mathbf{k} \in \mathbb{Z}^n} (1 + \|\mathbf{k}\|^{4\alpha}) |\hat{U}_{\mathbf{k}}|^2.$$

When  $\alpha = 0$ ,  $\|U\|_{X_0} = \|U\|_0 = \|U\|$ .

- $\text{QP}(\mathbb{R}^d)$  **space:** let  $\text{QP}(\mathbb{R}^d)$  be the space of all  $d$ -dimensional quasiperiodic functions.
- $L^q_{QP}(\mathbb{R}^d)$  **space:** for any fixed  $q \in [1, \infty)$ , denote

$$L^q_{QP}(\mathbb{R}^d) = \left\{ v(\mathbf{x}) \in \text{QP}(\mathbb{R}^d) : \|v\|_q^q = \int |v(\mathbf{x})|^q d\mathbf{x} < \infty \right\},$$

and

$$L^\infty_{QP}(\mathbb{R}^d) = \{v(\mathbf{x}) \in \text{QP}(\mathbb{R}^d) : \|v\|_\infty = \sup_{\mathbf{x} \in \mathbb{R}^d} |v(\mathbf{x})| < \infty\},$$

the inner product  $(\cdot, \cdot)_{L^2_{QP}(\mathbb{R}^d)}$

$$(v, w)_{L^2_{QP}(\mathbb{R}^d)} = \int v(\mathbf{x}) \bar{w}(\mathbf{x}) d\mathbf{x}.$$

By the Parseval identity (4), we have

$$\|v\|_{L^2_{QP}(\mathbb{R}^d)}^2 = \sum_{\lambda \in \sigma(v)} |\hat{v}_\lambda|^2.$$

- $\mathcal{C}_{QP}^\alpha(\mathbb{R}^d)$  **space:** the space  $\mathcal{C}_{QP}^\alpha(\mathbb{R}^d)$  consists of quasiperiodic functions with continuous derivatives up to order  $\alpha$  on  $\mathbb{R}^d$ . The  $\mathcal{C}_{QP}^\alpha$ -norm of  $v \in \mathcal{C}_{QP}^\alpha(\mathbb{R}^d)$  is defined by

$$\|v\|_{\mathcal{C}_{QP}^\alpha} = \sum_{|\mathbf{m}| \leq \alpha} \sup_{\mathbf{x} \in \mathbb{R}^d} |\partial_{\mathbf{x}}^{\mathbf{m}} v|.$$

- $H_{QP}^\alpha(\mathbb{R}^d)$  **space:** for any  $\alpha \in \mathbb{N}_0$ , the Hilbert space  $H_{QP}^\alpha(\mathbb{R}^d)$  comprises all quasiperiodic functions with partial derivatives order  $\alpha \geq 1$ . For  $v, w \in H_{QP}^\alpha(\mathbb{R}^d)$ , the inner product  $(\cdot, \cdot)_{H_{QP}^\alpha(\mathbb{R}^d)}$  is

$$(v, w)_{H_{QP}^\alpha(\mathbb{R}^d)} = (v, w)_{L^2_{QP}(\mathbb{R}^d)} + \sum_{|\mathbf{m}|=\alpha} (\partial_{\mathbf{x}}^{\mathbf{m}} v, \partial_{\mathbf{x}}^{\mathbf{m}} w)_{L^2_{QP}(\mathbb{R}^d)}.$$

The corresponding norm is

$$\|v\|_{H_{QP}^\alpha(\mathbb{R}^d)}^2 = \sum_{\lambda \in \sigma(v)} (1 + |\boldsymbol{\lambda}|^2)^\alpha |\hat{v}_\lambda|^2.$$

In particular, for  $\alpha = 0$ ,  $H_{QP}^0(\mathbb{R}^d) = L^2_{QP}(\mathbb{R}^d)$ . To simplify notation, we denote  $(\cdot, \cdot) = (\cdot, \cdot)_{L^2_{QP}(\mathbb{R}^d)}$  and  $(\cdot, \cdot)_\alpha = (\cdot, \cdot)_{H_{QP}^\alpha(\mathbb{R}^d)}$ . The embedding theorem of  $H_{QP}^\alpha(\mathbb{R}^d)$  can be found in [37].

A recent study has revealed an important relationship between quasiperiodic function and its parent function, see Lemma 3.1.

**Lemma 3.1** ([28]). *Consider a quasiperiodic function  $v(\mathbf{x}) = v_p(\mathbf{P}^T \mathbf{x})$  where  $v_p(\mathbf{y})$  is its parent function and  $\mathbf{P} \in \mathbb{P}^{d \times n}$ . Let the quasiperiodic Fourier coefficient  $\hat{v}_\lambda = (v, e^{i\boldsymbol{\lambda} \cdot \mathbf{x}})$  and the periodic Fourier coefficient  $\hat{v}_p(\mathbf{k}) = (v_p, e^{i\mathbf{k} \cdot \mathbf{y}})_{L^2(\mathbb{T}^n)}$ . Then, we have*

$$\hat{v}_\lambda = \hat{v}_p(\mathbf{k}),$$

where  $\boldsymbol{\lambda} = \mathbf{P}\mathbf{k}$ ,  $\mathbf{k} \in \mathbb{Z}^n$ .

Based on Lemma 3.1, we prove the norm inequality between quasiperiodic function and its parent function.

**Theorem 3.2.** *For any  $v \in QP(\mathbb{R}^d)$ , and  $v_p$  is the corresponding  $n$ -dimensional parent function. Assume that  $\alpha \geq s/2 > n/4$  and  $v_p \in X_\alpha$ . Then, the bound*

$$\|v\|_{L^\infty_{QP}(\mathbb{R}^d)} \leq C \|v_p\|_s \leq C \|v_p\|_{X_\alpha} \quad (18)$$

is valid and the following estimate

$$\|wv\|_{L^2_{QP}(\mathbb{R}^d)} \leq C \|w\|_{L^2_{QP}(\mathbb{R}^d)} \cdot \|v_p\|_{X_\alpha}, \quad w \in L^2_{QP}(\mathbb{R}^d), \quad v_p \in X_\alpha$$

holds where  $C$  is a constant.

*Proof.* Applying Lemma 3.1 and Cauchy-Schwarz inequality, we have

$$\begin{aligned} \sum_{j=1}^{\infty} |\hat{v}_{\lambda_j}| &= \sum_{j=1}^{\infty} \left[ |\hat{v}_p(\mathbf{k}_j)| (1 + |\mathbf{k}_j|^2)^{s/2} (1 + |\mathbf{k}_j|^2)^{-s/2} \right] \\ &\leq \sum_{j=1}^{\infty} \left[ |\hat{v}_p(\mathbf{k}_j)|^2 (1 + |\mathbf{k}_j|^2)^s \right] \sum_{j=1}^{\infty} (1 + |\mathbf{k}_j|^2)^{-s} \\ &= C \|v_p\|_s. \end{aligned}$$

The last estimate holds since  $s > n/2$  implies the series  $\sum_{j=1}^{\infty} (1 + |\mathbf{k}_j|^2)^{-s}$  converges. When the Fourier series of  $v$  is absolutely convergent, then it uniformly convergent to the quasiperiodic function  $v$  (Theorem 1.20 in [36]), such that  $\|v\|_{L_{QP}^{\infty}(\mathbb{R}^d)} \leq \sum_{j=1}^{\infty} |\hat{v}_{\lambda_j}|$ . Therefore, we have  $\|v\|_{L_{QP}^{\infty}(\mathbb{R}^d)} \leq C \|v_p\|_s$ , where  $C$  is a positive constant. Using the definition of  $\|\cdot\|_s$  and  $\|\cdot\|_{X_{\alpha}}$ , we can obtain

$$\|v_p\|_s \leq C \|v_p\|_{X_{2s}},$$

and for  $0 \leq \alpha_1 \leq \alpha_2$ ,

$$\|v_p\|_{X_{\alpha_1}} \leq \|v_p\|_{X_{\alpha_2}}.$$

Combining  $\alpha \geq s/2$ , it follows that  $\|v_p\|_s \leq C \|v_p\|_{X_{\alpha}}$ . Therefore, the inequality (18) holds. Further, for any  $w \in L_{QP}^2(\mathbb{R}^d)$ , we can obtain

$$\|vw\|_{L_{QP}^2(\mathbb{R}^d)} \leq \|w\|_{L_{QP}^2(\mathbb{R}^d)} \cdot \|v\|_{L_{QP}^{\infty}(\mathbb{R}^d)} \leq C \|w\|_{L_{QP}^2(\mathbb{R}^d)} \cdot \|v_p\|_{X_{\alpha}}.$$

□

## 3.2 Convergence analysis

This subsection presents the convergence analysis of full discretization scheme (16).

### 3.2.1 Main theorem

Let  $u_p^j$  denote the parent function of  $u^j$ , where  $u^j$  is the approximate solution at  $t = t_j$  exactly satisfying the scheme (12). Below, we give the main theorem of the error analysis of PM-OS2.

**Theorem 3.3.** *Let  $u(\cdot, t_m)$  and  $u_N^m$  be the solutions of problems (6) and (16) at  $t_m$ , respectively. Then under the conditions*

(i) *The potential  $V$  is a  $C^1$ -smooth function and  $\|V_p\|_{X_{\alpha}} \leq C_V$ ,  $\alpha \geq s/2 > n/4$ ;*

(ii) *The parent function  $u_p^j \in H^{\alpha}(\mathbb{T}^n)$ ,  $0 \leq j \leq m$ ;*

*the global error bound of PM-OS2 (16) is*

$$\|u_N^m - u(\cdot, t_m)\|_{L_{QP}^2(\mathbb{R}^d)} \leq C(\tau^2 + N^{-\alpha}).$$

The constant  $C > 0$  depends on the bounds  $C_V$ ,  $\sup\{\|u(\cdot, t)\|_{L^2_{QP}(\mathbb{R}^d)} : 0 \leq t \leq T\}$  and  $\max\{|u_p^j|_\alpha : 0 \leq j \leq m\}$ .

The detailed proof of Theorem 3.3 is given at the end of this section.

### 3.2.2 Some results

Before proving the main conclusion, we present some required results.

**Lemma 3.4.** *The operator  $A$  defined in (6) is self-adjoint in the inner product  $L^2_{QP}$ .*

*Proof.* When  $v, w \in \text{QP}(\mathbb{R}^d)$  and are differentiable, applying the Green identity, we have

$$\begin{aligned} (Av, w) - (v, Aw) &= -(\Delta v, w) + (v, \Delta w) \\ &= -\int \Delta v \cdot w \, d\mathbf{x} + \int v \cdot \Delta w \, d\mathbf{x} \\ &= -\lim_{L \rightarrow \infty} \frac{1}{|\Omega_L|} \int_{\partial\Omega_L} \frac{\partial v}{\partial \mathbf{n}} \cdot w \, dS + \lim_{L \rightarrow \infty} \frac{1}{|\Omega_L|} \int_{\partial\Omega_L} v \cdot \frac{\partial w}{\partial \mathbf{n}} \, dS, \end{aligned}$$

where  $\mathbf{n}$  is the outward normal of  $\partial\Omega_L$ . Since the quasiperiodic functions  $v, w$  are bounded, i.e.,  $\sup_{\mathbf{x} \in \mathbb{R}^d} \{v(\mathbf{x}), w(\mathbf{x})\} \leq C < \infty$ , it follows that

$$\left| \lim_{L \rightarrow \infty} \frac{1}{|\Omega_L|} \int_{\partial\Omega_L} \frac{\partial v}{\partial \mathbf{n}} \cdot w \, dS \right| \leq \lim_{L \rightarrow \infty} \frac{C^2 2d(2L)^{d-1}}{(2L)^d} = 0, \quad \left| \lim_{L \rightarrow \infty} \frac{1}{|\Omega_L|} \int_{\partial\Omega_L} v \cdot \frac{\partial w}{\partial \mathbf{n}} \, dS \right| = 0.$$

Therefore,  $(-\Delta v, w) = (v, -\Delta w)$  is true. The proof of this theorem is completed.  $\square$

We recall some basic definitions that occur in the following.

**Definition 3.5.** *The operator  $B$  is unitary if  $BB^* = B^*B = \mathcal{I}$ , where  $\mathcal{I}$  is the identity operator and  $B^*$  is adjoint operator of  $B$ .*

**Definition 3.6.** *A one-parametric family  $\Psi(t), t \in \mathbb{R}$ , of linear operators on a Banach space  $X$  is a group of operators on  $X$  if  $\Psi(0) = \mathcal{I}$  and  $\Psi(t+s) = \Psi(t)\Psi(s), s \in \mathbb{R}$ . Moreover,  $\Psi(t)$  is  $C_0$ -group if  $\lim_{t \rightarrow 0} \Psi(t)x = x$ , for all  $x \in X$ .*

**Lemma 3.7** (Stone Theorem [38]). *Let  $H$  be a Hilbert space, and  $\Psi(t)$  be a one-parameter family of linear operators on  $H$  for  $t \in \mathbb{R}$ .*

(i) *If  $\Psi(t)$  is  $C_0$ -group of unitary operators on  $H$ , then there exists a unique self-adjoint operator  $A$  such that  $\Psi(t) = e^{-itA}$ , where  $-iA$  is the generator.*

(ii) *Conversely, let  $A$  be a self-adjoint operator on  $H$ . Then  $\Psi(t) = e^{-itA}$  is a  $C_0$ -group of unitary operator with the generator  $-iA$ .*

Lemma 3.4 and Lemma 3.7 demonstrate  $\|e^{-itA}\|_{L^2_{QP}(\mathbb{R}^d)} = 1$ . Next, we will give an error bound of OS2 method (12) for TQSE (6). For operators  $A$  and  $B$ , we denote the commutators  $[A, B] = AB - BA$  and  $[A, [A, B]] = A^2B - 2ABA + BA^2$ .

**Lemma 3.8** (Theorem 2.1, [2]). *Suppose that the operators  $\Phi$  and  $\Psi$  are self-adjoint on the Hilbert space  $L^2_{QP}(\mathbb{R}^d)$ .*

(1) *Under the following conditions*

(i)  *$\Psi$  is bounded, i.e.,  $\|\Psi v\|_{L^2_{QP}(\mathbb{R}^d)} \leq \beta \|v\|_{L^2_{QP}(\mathbb{R}^d)}$ , where  $\beta$  is a constant and  $v \in L^2_{QP}(\mathbb{R}^d)$ .*

(ii) Commutator bound  $\|[\Phi, \Psi]v\|_{L^2_{QP}(\mathbb{R}^d)} \leq c_1 \|v\|_{H^1_{QP}}, \forall v \in H^1_{QP}(\mathbb{R}^d)$ .

We have

$$\|e^{-\frac{i}{2}\tau\Psi} e^{-i\tau\Phi} e^{-\frac{i}{2}\tau\Psi} v - e^{-i\tau(\Phi+\Psi)} v\|_{L^2_{QP}(\mathbb{R}^d)} \leq C_1 \tau^2 \|v\|_{L^2_{QP}(\mathbb{R}^d)},$$

where  $C_1$  depends only on  $c_1$  and  $\beta$ .

(2) Under the conditions in (1) and additionally

(iii) Commutator bound  $\|[\Phi, [\Phi, \Psi]]v\|_{L^2_{QP}(\mathbb{R}^d)} \leq c_2 \|v\|_{L^2_{QP}(\mathbb{R}^d)}, \forall v \in L^2_{QP}(\mathbb{R}^d)$ .

We have

$$\|e^{-\frac{i}{2}\tau\Psi} e^{-i\tau\Phi} e^{-\frac{i}{2}\tau\Psi} v - e^{-i\tau(\Phi+\Psi)} v\|_{L^2_{QP}(\mathbb{R}^d)} \leq C_2 \tau^3 \|v\|_{L^2_{QP}(\mathbb{R}^d)},$$

where  $C_2$  depends only on  $c_1, c_2$  and  $\beta$ .

**Theorem 3.9.** For a quasiperiodic function  $V$ , the following conclusions are valid.

(i) If  $V \in \mathcal{C}^2_{QP}(\mathbb{R}^d)$ , then  $\|\mathcal{S}v - \mathcal{T}v\|_{L^2_{QP}(\mathbb{R}^d)} \leq C\tau^2 \|v\|_{L^2_{QP}(\mathbb{R}^d)}$ .

(ii) If  $V \in \mathcal{C}^1_{QP}(\mathbb{R}^d)$ , we have  $\|\mathcal{S}v - \mathcal{T}v\|_{L^2_{QP}(\mathbb{R}^d)} \leq C\tau^3 \|v\|_{L^2_{QP}(\mathbb{R}^d)}$ .

*Proof.* According to Lemma 3.4, the operator  $A = -\Delta$  is self-adjoint in the sense of  $L^2_{QP}$ -norm. Next, we verify that the operators  $A$  and  $V$  satisfy commutator bounds. From the equation

$$\Delta(\phi\psi) = (\Delta\phi)\psi + 2(\nabla\phi)(\nabla\psi) + \phi(\Delta\psi),$$

we have

$$\|[\Delta, V]\phi\|_{L^2_{QP}(\mathbb{R}^d)} \leq \|(\Delta V)\phi\|_{L^2_{QP}(\mathbb{R}^d)} + 2\|(\nabla V) \cdot (\nabla\phi)\|_{L^2_{QP}(\mathbb{R}^d)} \leq C(\|V\|_{\mathcal{C}^2_{QP}}, \|\phi\|_1),$$

and

$$\|[V, [V, \Delta]]\phi\|_{L^2_{QP}(\mathbb{R}^d)} = \|2(\nabla V)(\nabla V)\phi\|_{L^2_{QP}(\mathbb{R}^d)} \leq C(\|V\|_{\mathcal{C}^1_{QP}}, \|\phi\|).$$

Combining with the conclusions in Lemma 3.8, these conclusions in this theorem are easy to prove.  $\square$

To prove the difference between  $\mathcal{S}_N$  and  $I_N \mathcal{S}$ , we first introduce the following lemmas.

**Lemma 3.10.** It holds

$$\|(I_N e^{-\frac{i}{2}\tau A} - e^{-\frac{i}{2}\tau A} I_N)v\|_{L^2_{QP}(\mathbb{R}^d)} \leq \int_0^\tau \| [A, I_N - \mathcal{I}] e^{-\frac{i}{2}tA} v \|_{L^2_{QP}(\mathbb{R}^d)} dt.$$

*Proof.* Consider the following two initial value problems

$$\begin{cases} \frac{d}{d\tau} u(\tau) = -\frac{i}{2} A u(\tau), \\ u(0) = v, \end{cases} \quad \text{and} \quad \begin{cases} \frac{d}{d\tau} w(\tau) = -\frac{i}{2} A w(\tau), \\ w(0) = I_N v. \end{cases}$$

For the initial value problem

$$\frac{d}{d\tau}(w - I_N u)(\tau) = -\frac{i}{2}Aw(\tau) - I_N(-\frac{i}{2}A)u(\tau), \quad (19)$$

with initial value  $(w - I_N u)(0) = 0$ , we have

$$(w - I_N u)(\tau) = e^{-\frac{i}{2}\tau A}I_N v - I_N e^{-\frac{i}{2}\tau A}v.$$

We rewrite (19) as

$$\frac{d}{d\tau}(w - I_N u)(\tau) = -\frac{i}{2}A(w - I_N u)(\tau) - \frac{i}{2}AI_N u(\tau) - I_N(-\frac{i}{2}A)u(\tau).$$

Applying the linear variation-of-constants formula, we obtain

$$\begin{aligned} (w - I_N u)(\tau) &= e^{-\frac{i}{2}A\tau}(w - I_N u)(0) + \int_0^\tau e^{-\frac{i}{2}A(t-\tau)}[-\frac{i}{2}A, I_N]e^{-\frac{i}{2}tA}v dt \\ &= \int_0^\tau e^{-\frac{i}{2}A(t-\tau)}[-\frac{i}{2}A, I_N - \mathcal{I}]e^{-\frac{i}{2}tA}v dt. \end{aligned} \quad (20)$$

For any  $v \in L^2_{QP}(\mathbb{R}^d)$ , applying Lemma 3.7, it follows that

$$\|e^{-\frac{i}{2}\tau A}v\|_{L^2_{QP}(\mathbb{R}^d)} = \|v\|_{L^2_{QP}(\mathbb{R}^d)}, \quad (21)$$

then  $(e^{-\frac{i}{2}\tau A})_{\tau \in \mathbb{R}}$  on  $L^2_{QP}(\mathbb{R}^d)$  is a unitary group. Combining with the formula (20), this completes the proof.  $\square$

**Lemma 3.11.** *Assume that there exists a constant  $C_V > 0$  such that  $\|V_p\|_{X_\alpha} \leq C_V$ . Then we have*

$$\|I_N e^{-i\tau V}v\|_{L^2_{QP}(\mathbb{R}^d)} \leq e^{CC_V\tau} \|I_N v\|_{L^2_{QP}(\mathbb{R}^d)}, \quad v \in L^2_{QP}(\mathbb{R}^d),$$

where  $\tau \in [0, T]$  and  $C$  is a constant.

*Proof.* Consider the problem

$$I_N \frac{d}{d\tau}u(\tau) = I_N(-iV)u(\tau), \quad \tau \in [0, T], \quad (22)$$

with initial value  $I_N u(0) = I_N v$ . We can obtain

$$I_N u(\tau) = I_N e^{-i\tau V}v.$$

For any  $v_1 \in L^\infty_{QP}(\mathbb{Q}_N)$ ,  $v_2 \in L^2_{QP}(\mathbb{R}^d)$ , assume that  $v_{p_1} \in X_\alpha$  is the parent function of  $v_1$ . Using Theorem 3.2, we have

$$\|I_N(v_1 v_2)\|_{L^2_{QP}(\mathbb{R}^d)} \leq \|v_1\|_{L^\infty_{QP}(\mathbb{Q}_N)} \|I_N v_2\|_{L^2_{QP}(\mathbb{R}^d)} \leq C \|v_{p_1}\|_{X_\alpha} \|I_N v_2\|_{L^2_{QP}(\mathbb{R}^d)}.$$

Integrating (22) from 0 to  $\tau$  yields

$$\begin{aligned}
\|I_N u\|_{L^2_{QP}(\mathbb{R}^d)} &\leq \|I_N v\|_{L^2_{QP}(\mathbb{R}^d)} + \int_0^\tau \|I_N V u(t)\|_{L^2_{QP}(\mathbb{R}^d)} dt \\
&\leq \|I_N v\|_{L^2_{QP}(\mathbb{R}^d)} + C \|V_p\|_{X_\alpha} \int_0^\tau \|I_N u\|_{L^2_{QP}(\mathbb{R}^d)} dt \\
&\leq \|I_N v\|_{L^2_{QP}(\mathbb{R}^d)} + CC_V \int_0^\tau \|I_N u\|_{L^2_{QP}(\mathbb{R}^d)} dt.
\end{aligned}$$

Then we can prove the theorem by applying the Gronwall inequality.  $\square$

The error analysis of PM in the sense of  $L^2_{QP}$ -norm is as follows.

**Lemma 3.12** ([28]). *Suppose that  $u(\mathbf{x}) \in QP(\mathbb{R}^d)$  and its parent function  $u_p(\mathbf{y}) \in H^\alpha(\mathbb{T}^n)$  with  $\alpha > n/2$ . There exists a constant  $C$ , independent of  $u_p$  and  $N$ , such that*

$$\|I_N u - u\|_{L^2_{QP}(\mathbb{R}^d)} \leq CN^{-\alpha} |u_p|_\alpha.$$

Now, we analyze the difference between  $\mathcal{S}_N$  and  $I_N \mathcal{S}$ . Let  $u_p$ ,  $v_p$  and  $w_p$  be the parent functions of quasiperiodic functions  $u$ ,  $v$  and  $w$ , respectively.

**Theorem 3.13.** *For  $u \in QP(\mathbb{R}^d)$ ,  $v = Su$  and  $w = e^{-\frac{i}{2}\tau A} u$ . Assume that  $\|V_p\|_{X_\alpha} \leq C_V$  and  $u_p, v_p, w_p \in H^\alpha(\mathbb{T}^n)$  with  $\alpha \geq s/2 > n/4$ . Then we have*

$$\|\mathcal{S}_N(u) - I_N \mathcal{S}(u)\|_{L^2_{QP}(\mathbb{R}^d)} \leq C\tau N^{-\alpha} (|v_p|_\alpha + |w_p|_\alpha),$$

where  $C$  is a constant.

*Proof.* Since

$$\begin{aligned}
I_N \mathcal{S}(u) - \mathcal{S}_N(u) &= I_N e^{-\frac{i}{2}\tau A} e^{-i\tau V} e^{-\frac{i}{2}\tau A} u - e^{-\frac{i}{2}\tau A} I_N e^{-i\tau V} I_N e^{-\frac{i}{2}\tau A} I_N u \\
&= I_N e^{-\frac{i}{2}\tau A} e^{-i\tau V} e^{-\frac{i}{2}\tau A} u - e^{-\frac{i}{2}\tau A} I_N e^{-i\tau V} e^{-\frac{i}{2}\tau A} u \\
&\quad + e^{-\frac{i}{2}\tau A} I_N e^{-i\tau V} e^{-\frac{i}{2}\tau A} u - e^{-\frac{i}{2}\tau A} I_N e^{-i\tau V} I_N e^{-\frac{i}{2}\tau A} u \\
&\quad + e^{-\frac{i}{2}\tau A} I_N e^{-i\tau V} I_N e^{-\frac{i}{2}\tau A} u - e^{-\frac{i}{2}\tau A} I_N e^{-i\tau V} I_N e^{-\frac{i}{2}\tau A} I_N u \\
&= Z_1 + Z_2 + Z_3.
\end{aligned}$$

Then we estimate the bounds of  $\|Z_1\|_{L^2_{QP}(\mathbb{R}^d)}$ ,  $\|Z_2\|_{L^2_{QP}(\mathbb{R}^d)}$  and  $\|Z_3\|_{L^2_{QP}(\mathbb{R}^d)}$ , respectively.

(i) For  $Z_1$  and using Lemma 3.10, we have

$$\begin{aligned}
\|Z_1\|_{L^2_{QP}(\mathbb{R}^d)} &= \|(I_N e^{-\frac{i}{2}\tau A} - e^{-\frac{i}{2}\tau A} I_N) e^{-i\tau V} e^{-\frac{i}{2}\tau A} u\|_{L^2_{QP}(\mathbb{R}^d)} \\
&\leq \int_0^\tau \|[A(I_N - \mathcal{I}) - (I_N - \mathcal{I})A] e^{-\frac{i}{2}tA} e^{-itV} e^{-\frac{i}{2}tA} u\|_{L^2_{QP}(\mathbb{R}^d)} dt \\
&= \int_0^\tau \|[A(I_N - \mathcal{I}) - (I_N - \mathcal{I})A] v\|_{L^2_{QP}(\mathbb{R}^d)} dt
\end{aligned}$$

where  $v = \mathcal{S}u$ . Since  $|v_p|_\alpha < +\infty$ , applying Lemma 3.12, it follows that

$$\|Z_1\|_{L^2_{QP}(\mathbb{R}^d)} \leq C\tau N^{-\alpha}|v_p|_\alpha.$$

(ii) For  $Z_2$ , using (21) and Lemma 3.11, we have

$$\begin{aligned} \|Z_2\|_{L^2_{QP}(\mathbb{R}^d)} &= \|e^{-\frac{i}{2}\tau A} I_N e^{-i\tau V} (e^{-\frac{i}{2}\tau A} u - I_N e^{-\frac{i}{2}\tau A} u)\|_{L^2_{QP}(\mathbb{R}^d)} \\ &= \|I_N e^{-i\tau V} (e^{-\frac{i}{2}\tau A} u - I_N e^{-\frac{i}{2}\tau A} u)\|_{L^2_{QP}(\mathbb{R}^d)} \\ &\leq e^{CC_V\tau} \|I_N (e^{-\frac{i}{2}\tau A} u - I_N e^{-\frac{i}{2}\tau A} u)\|_{L^2_{QP}(\mathbb{R}^d)} = 0. \end{aligned}$$

(iii) For  $Z_3$ , using (21), Lemma 3.10 and Lemma 3.11, we have

$$\begin{aligned} \|Z_3\|_{L^2_{QP}(\mathbb{R}^d)} &= \|e^{-\frac{i}{2}\tau A} I_N e^{-i\tau V} (I_N e^{-\frac{i}{2}\tau A} u - I_N e^{-\frac{i}{2}\tau A} I_N u)\|_{L^2_{QP}(\mathbb{R}^d)} \\ &\leq e^{CC_V\tau} \|I_N (I_N e^{-\frac{i}{2}\tau A} u - I_N e^{-\frac{i}{2}\tau A} I_N u)\|_{L^2_{QP}(\mathbb{R}^d)} \\ &= e^{CC_V\tau} \|(I_N e^{-\frac{i}{2}\tau A} - e^{-\frac{i}{2}\tau A} I_N)u\|_{L^2_{QP}(\mathbb{R}^d)} \\ &\leq e^{CC_V\tau} \int_0^\tau \|[A, I_N - \mathcal{I}]e^{-\frac{i}{2}tA}u\|_{L^2_{QP}(\mathbb{R}^d)} dt \\ &\leq C\tau N^{-\alpha}|w_p|_\alpha. \end{aligned}$$

□

### 3.2.3 The proof of Theorem 3.3

Using the triangle inequality, we have

$$\|u_N^m - u(\cdot, t_m)\|_{L^2_{QP}(\mathbb{R}^d)} \leq \|u_N^m - u^m\|_{L^2_{QP}(\mathbb{R}^d)} + \|u^m - u(\cdot, t_m)\|_{L^2_{QP}(\mathbb{R}^d)},$$

where  $u^m$  is the splitting solution of the scheme (12) at  $t = t_m$  with  $u^0 = u_0$ . We now apply the Lady Windermere's fan to represent the global errors as follows

$$\begin{aligned} u^m - u(\cdot, t_m) &= \mathcal{S}^m u_0 - \mathcal{T}^m u_0 = \sum_{j=0}^{m-1} \mathcal{S}^{m-j-1} (\mathcal{S} - \mathcal{T}) \mathcal{T}^j u_0, \\ u_N^m - u^m &= \mathcal{S}_N^m u_0 - \mathcal{S}^m u_0 = (I_N - \mathcal{I})u^m + \sum_{j=1}^m \mathcal{S}_N^{m-j} (\mathcal{S}_N(u^{j-1}) - I_N \mathcal{S}(u^{j-1})). \end{aligned}$$

Applying Theorem 3.9, we have

$$\begin{aligned} \|u^m - u(\cdot, t_m)\|_{L^2_{QP}(\mathbb{R}^d)} &= \left\| \sum_{j=0}^{m-1} \mathcal{S}^{m-j-1} (\mathcal{S} - \mathcal{T}) \mathcal{T}^j u_0 \right\|_{L^2_{QP}(\mathbb{R}^d)} \\ &\leq \sum_{j=0}^{m-1} \|\mathcal{S} - \mathcal{T}\|_{L^2_{QP}(\mathbb{R}^d)} \cdot \|\mathcal{T}^j u_0\|_{L^2_{QP}(\mathbb{R}^d)} \end{aligned}$$



$$\leq C\tau^2 \sup_{0 \leq t \leq T} \|u(\cdot, t)\|_{L^2_{QP}(\mathbb{R}^d)}.$$

Considering the regularity of the solution, then

$$\begin{aligned} \|u_N^m - u^m\|_{L^2_{QP}(\mathbb{R}^d)} &\leq \|(I_N - \mathcal{I})u^m\|_{L^2_{QP}(\mathbb{R}^d)} + \left\| \sum_{j=1}^m \mathcal{S}_N^{m-j} (\mathcal{S}_N(u^{j-1}) - I_N \mathcal{S}(u^{j-1})) \right\|_{L^2_{QP}(\mathbb{R}^d)} \\ &\leq CN^{-\alpha} |u_p^m|_\alpha + \sum_{j=1}^m e^{CC_V(m-j)\tau} \|\mathcal{S}_N(u^{j-1}) - I_N \mathcal{S}(u^{j-1})\|_{L^2_{QP}(\mathbb{R}^d)} \\ &\leq CN^{-\alpha} |u_p^m|_\alpha + Cm\tau N^{-\alpha} \max_{0 \leq j \leq m-1} |u_p^j|_\alpha \\ &\leq CN^{-\alpha} \max_{0 \leq j \leq m} |u_p^j|_\alpha. \end{aligned}$$

Therefore, the desired result can be directly obtained from the above two estimates.

The above analysis framework of the PM-OS2 is also applicable to the QSM-OS2, also showing exponential convergence in space and second-order accuracy in time. Besides, since QSM is essentially a generalization of Fourier spectral method, we can offer another way to analyze QSM. Concretely, similar to the analytical framework of Fourier spectral method to solve the Schrödinger equation with periodic potentials [2], we give the error analysis of QSM-OS2 based on the embedding theorem of quasiperiodic function space, see Appendix A for details.

## 4 Numerical Results

In this section, we provide some numerical experiments to verify the accuracy and performance of QSM-OS2 and PM-OS2 for solving TQSE (1). In the following numerical results, we only show the quasiperiodic structure in finite domain. It also should be emphasized that the developed methods have obtained global quasiperiodic solution over  $\mathbb{R}^d$ . All algorithms are implemented using MSVC++ 14.29 on Visual Studio Community 2019. The software of FFTW 3.3.5 is used to compute FFT [39]. All computations are performed on a workstation with an Intel Core 2.30GHz CPU, 16GB RAM. Let CPU(s) denote the computational time in seconds. For QSM-OS2, let  $k = 5$  in (17).

We use  $L^2_{QP}$ -norm to measure the numerical error

$$\text{Err}_h^\tau = \|u_N^m - u(\cdot, t_m)\|_{L^2_{QP}(\mathbb{R}^d)},$$

where  $\tau$  is the time step size and  $h$  is the mesh size of the  $n$ -dimensional torus. The error order in time direction is calculated by

$$\text{Ord} = \frac{\ln(\text{Err}_h^{\tau_1} / \text{Err}_h^{\tau_2})}{\ln(\tau_1 / \tau_2)}.$$

Our numerical examples focus on verifying the accuracy in space direction and the error order in time direction. As a result, the final time  $T$  can be arbitrarily chosen. For simplicity, we choose  $T = 0.001$ .

## 4.1 One-dimensional case

Consider one dimensional TQSE (1) with the incommensurate potential

$$V(x) = 2(\cos x + \cos \sqrt{3}x),$$

and initial value

$$u_0(x) = \sum_{\lambda \in \sigma(u_0)} \hat{u}_\lambda e^{i\lambda x},$$

where  $\hat{u}_\lambda = e^{-(|m_1|+|m_2|)}$  and  $\sigma(u_0) = \{\lambda = m_1 + m_2\sqrt{3} : m_1, m_2 \in \mathbb{Z}, -32 \leq m_1, m_2 \leq 31\}$ .

The reference solution on  $\mathbb{R}$  is obtained by using PM-OS2 with the time step size  $\tau = 1 \times 10^{-8}$  and the mesh size of the two-dimensional torus  $h = \pi/128$  in each direction. Figure 1 only shows the distribution of the probability density function  $|u(x, T)|^2$  in  $x \in [0, 240\pi]$  and corresponding diffraction pattern of the reference solution, respectively. In the right plot of Figure 1, we can see that the dots of different colors are constantly alternating and the distribution Fourier exponent has rotational symmetry but no translational symmetry.

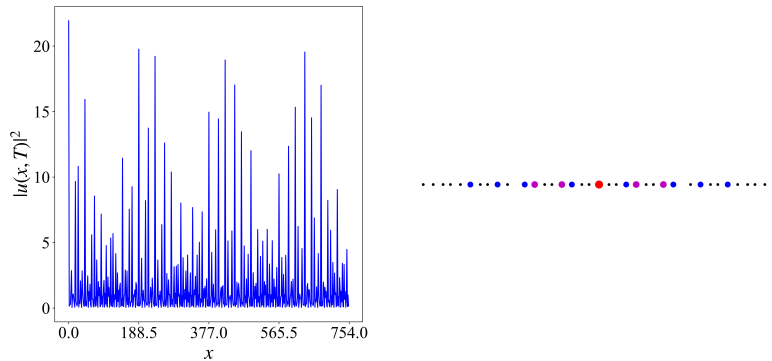


**Fig. 1:** The reference solution of one-dimensional TQSE. Left: Probability density distribution  $|u(x, T)|^2$ ,  $x \in [0, 240\pi]$ . Right: Distribution of Fourier exponents  $\lambda$  when  $|\hat{u}_\lambda| > 8.620e-02$ . We arrange the values of  $|\hat{u}_\lambda|$  from largest to smallest, then red, purple and blue dots represent the order of  $|\hat{u}_\lambda|$  at the corresponding Fourier exponents from the largest to the smallest, respectively.

We first show the convergence rate when solving TQSE using PM and QSM in space direction. Set the time step size  $\tau = 1 \times 10^{-6}$ , Table 1 shows numerical error  $\text{Err}_h^\tau$  and the required CPU time of PM-OS2 and QSM-OS2, respectively. We find that  $\text{Err}_h^\tau$  decays exponentially as  $N$  increases due to the smoothness of wave function  $u(x, t)$ . Meanwhile, the CPU time of PM is less than that of QSM since PM can use 2D FFT. Figure 2 further details CPU time of both methods as  $N$  increases.

**Table 1:** Numerical error  $\text{Err}_h^\tau$  and CPU time of PM-OS2 and QSM-OS2 for different  $N$  and  $\tau = 1 \times 10^{-6}$ .

	$N \times N$	$2 \times 2$	$4 \times 4$	$8 \times 8$	$16 \times 16$	$32 \times 32$
$\text{Err}_h^\tau$	PM-OS2	2.784e-03	5.091e-04	1.696e-05	1.137e-08	2.488e-12
	QSM-OS2	3.335e-03	5.430e-04	1.748e-05	1.153e-08	2.485e-12

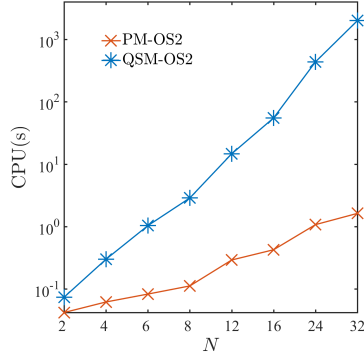


**Fig. 2:** CPU time between PM-OS2 and QSM-OS2 against  $N$ .

Next, we verify the error order of applying OS2 method to solve TQSE in time direction. Meanwhile, we choose  $h = \pi/128$  to make the approximation error in space direction that does not affect the error in time direction. From the numerical results shown in Table 1, PM-OS2 and QSM-OS2 have the same convergence rate in space direction, while the PM-OS2 is more efficient in CPU time. Therefore, the time error of both methods is the same and we only present the temporal error of PM-OS2, see Table 2.

**Table 2:** Temporal error test of PM-OS2 with  $h = \pi/128$ .

$\tau$	$1 \times 10^{-3}$	$5 \times 10^{-4}$	$2.5 \times 10^{-4}$	$1.25 \times 10^{-4}$
$\text{Err}_h^\tau$	1.608e-09	4.021e-10	1.005e-10	2.513e-11
Ord	-	2.00	2.00	2.00

## 4.2 Two-dimensional cases

In this subsection, we further demonstrate that the PM is a high-precision and efficient algorithm to solve TQSE through the two-dimensional example. Consider the potential function

$$V(\mathbf{x}) = \sum_{j=1}^5 e^{i(\mathbf{P}_1 \mathbf{k}_j) \cdot \mathbf{x}} - e^{i(\mathbf{P}_1 \mathbf{k}_6) \cdot \mathbf{x}}, \quad \mathbf{x} \in \mathbb{R}^2,$$

where

$$(\mathbf{k}_1, \mathbf{k}_2, \mathbf{k}_3, \mathbf{k}_4, \mathbf{k}_5, \mathbf{k}_6) = \begin{pmatrix} 0 & 0 & 1 & 0 & 0 & 0 \\ 1 & -1 & 0 & 0 & 0 & 0 \\ 0 & 0 & 0 & 0 & 1 & -1 \\ 0 & 0 & 0 & 1 & 0 & 0 \end{pmatrix},$$

and the corresponding projection matrix

$$\mathbf{P}_1 = \begin{pmatrix} 1 & \cos(\pi/4) & 0 & -\cos(\pi/4) \\ 0 & \sin(\pi/4) & 1 & \sin(\pi/4) \end{pmatrix}.$$

Therefore, this quasiperiodic system can be embedded into a four-dimensional parent system. Let the initial value

$$u_0(\mathbf{x}) = \sum_{\boldsymbol{\lambda} \in \sigma_1(u_0)} e^{-(|\mathbf{k}_1|+|\mathbf{k}_2|+|\mathbf{k}_3|+|\mathbf{k}_4|)} e^{i\boldsymbol{\lambda} \cdot \mathbf{x}}, \quad \boldsymbol{\lambda} = \mathbf{P}_1 \mathbf{k},$$

where  $\sigma_1(u_0) = \{\boldsymbol{\lambda} = \mathbf{P}_1 \mathbf{k} : k_1, k_2, k_3, k_4 \in \mathbb{Z}, -16 \leq k_1, k_2, k_3, k_4 \leq 15\}$ .

The reference solution on  $\mathbb{R}^2$  is given by PM-OS2 under  $\tau = 1 \times 10^{-7}$  and the mesh size of the four-dimensional torus  $h = \pi/64$  in each direction. In Figure 3, we present the distribution of the probability density function  $|u(\mathbf{x}, T)|^2$  and the corresponding diffraction pattern of the reference solution, respectively. The structure shown in Figure 3 is a typical octagonal quasicrystal. The reciprocal space, shown on the right plot of Figure 3, indicates octagonal rotational symmetry.

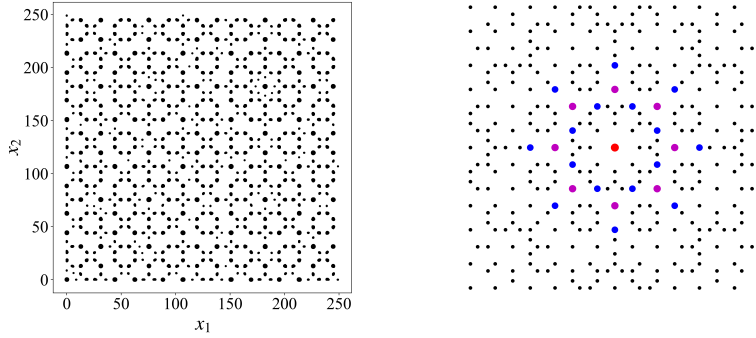


**Fig. 3:** The reference solution of two-dimensional TQSE. Left: Probability density distribution  $|u(\mathbf{x}, T)|^2$ ,  $\mathbf{x} \in [0, 80\pi]^2$ . Right: Distribution of Fourier exponents  $\boldsymbol{\lambda}$  when  $|\hat{u}_{\boldsymbol{\lambda}}| > 23.970$ . By arranging the values of  $|\hat{u}_{\boldsymbol{\lambda}}|$  from largest to smallest, red, purple and blue dots represent the distribution of Fourier exponents corresponding to the first, first nine and first twenty-five values of  $|\hat{u}_{\boldsymbol{\lambda}}|$ , respectively.

Table 3 shows the numerical error  $\text{Err}_h^\tau$  and CPU time of PM-OS2. Obviously, the PM-OS2 has exponential convergence. When the fine mesh size  $h = \pi/16$ , the numerical error in space does not affect the error in time direction. Table 4 verifies that the PM-OS2 has second-order error accuracy in time direction with  $h = \pi/16$ .

**Table 3:** Numerical error  $\text{Err}_h^\tau$  and CPU time of PM-OS2 for different  $N$ .

$N \times N \times N \times N$	$4 \times 4 \times 4 \times 4$	$8 \times 8 \times 8 \times 8$	$16 \times 16 \times 16 \times 16$	$32 \times 32 \times 32 \times 32$
$\text{Err}_h^\tau$	3.881e-03	4.830e-04	9.936e-09	7.174e-13
CPU(s)	0.132	1.537	32.217	663.971

**Table 4:** Temporal error test of PM-OS2 with  $h = \pi/16$ .

$\tau$	$1 \times 10^{-3}$	$5 \times 10^{-4}$	$2.5 \times 10^{-4}$	$1.25 \times 10^{-4}$
$\text{Err}_h^\tau$	5.230e-10	1.308e-10	3.281e-11	8.667e-12
Ord	-	2.00	1.99	1.92

Furthermore, by changing the projection matrix and the initial value, we can obtain different quasicrystal. Let projection matrix be

$$\mathbf{P}_2 = \begin{pmatrix} 1 & \cos(\pi/6) & \cos(\pi/3) & 0 \\ 0 & \sin(\pi/6) & \sin(\pi/3) & 1 \end{pmatrix},$$

and initial value be

$$u_0(\mathbf{x}) = \sum_{\lambda \in \sigma_2(u_0)} e^{-\|\lambda\|^2} e^{i\lambda \cdot \mathbf{x}},$$

where  $\sigma_2(u_0) = \{\boldsymbol{\lambda} = \mathbf{P}_2 \mathbf{k} : k_1, k_2, k_3, k_4 \in \mathbb{Z}, -8 \leq k_1, k_2, k_3, k_4 \leq 7\}$ , we can obtain the dodecagonal quasicrystal as shown in Figure 4 under the time step size  $\tau = 1 \times 10^{-7}$  and the mesh size  $h = \pi/32$  of the four-dimensional torus.

## 5 Conclusions

In this paper, two high-accuracy numerical methods, the QSM-OS2 and PM-OS2, have been developed to solve arbitrary dimensional TQSE (1) and to obtain global quasiperiodic solutions. A rigorous convergence analysis shows that QSM-OS2 and PM-OS2 have exponential convergence in space when the potential function has enough regularity and second-order accuracy in time. Meanwhile the computational complexity analysis demonstrates that the PM-OS2 is more efficient than the QSM-OS2. The one- and two-dimensional numerical experiments further verify the theoretical results.

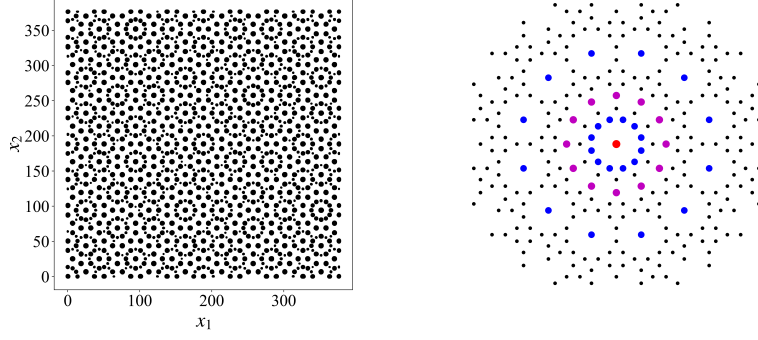


**Fig. 4:** The reference solution of two-dimensional TQSE. Left: Probability density distribution  $|u(\mathbf{x}, T)|^2$ ,  $\mathbf{x} \in [0, 120\pi]^2$ . Right: Distribution of Fourier exponents  $\lambda$  when  $|\hat{u}_\lambda| > 0.044$ . We arrange the values of  $|\hat{u}_\lambda|$  from largest to smallest, then red, purple and blue dots represent the distribution of Fourier exponents corresponding to the first, first thirteen and first thirty-seven values of  $|\hat{u}_\lambda|$ , respectively.

## Appendix A Another way to analyze QSM-OS2

The QSM is an extension of Fourier spectral method. Based on the embedding theorem of the quasiperiodic function given below, we can give the convergence analysis of QSM-OS2. Firstly, we give the following embedding theorem. Similar to the definition of  $X_\alpha$  on a torus  $\mathbb{T}^n$ , we define the quasiperiodic function space  $\mathcal{X}_\alpha$  on  $\mathbb{R}^d$

$$\mathcal{X}_\alpha = \left\{ f(\mathbf{x}) = \sum_{\lambda \in \sigma(f)} \hat{f}_\lambda e^{i\lambda \cdot \mathbf{x}} \in L^2_{QP}(\mathbb{R}^d) : \|(-\Delta)^\alpha f\|^2 = \sum_{\lambda \in \sigma(f)} |\hat{f}_\lambda|^2 \cdot \|\lambda\|^{4\alpha} < \infty \right\}.$$

**Theorem A.1.** For any  $f \in QP(\mathbb{R}^d)$ . Assume that  $\alpha \geq s/2 > d/4$ . Then, the bound

$$\|f\|_{L^\infty_{QP}(\mathbb{R}^d)} \leq C \|f\|_s \leq C \|f\|_{\mathcal{X}_\alpha}$$

is valid and the following estimate

$$\|wf\|_{L^2_{QP}(\mathbb{R}^d)} \leq C \|w\|_{L^2_{QP}(\mathbb{R}^d)} \cdot \|f\|_{\mathcal{X}_\alpha}, \quad w \in L^2_{QP}(\mathbb{R}^d), \quad f \in \mathcal{X}_\alpha$$

holds where  $C$  is a constant.

*Proof.* By the Hölder inequality, we have

$$\begin{aligned} \sum_{j=1}^p |\hat{f}_{\lambda_j}| &= \sum_{j=1}^p |\hat{f}_{\lambda_j}| \cdot (1 + |\lambda_j|^2)^{s/2} \cdot (1 + |\lambda_j|^2)^{-s/2} \\ &\leq \left( \sum_{j=1}^p |\hat{f}_{\lambda_j}|^2 (1 + |\lambda_j|^2)^s \right)^{\frac{1}{2}} \cdot \left( \sum_{j=1}^p (1 + |\lambda_j|^2)^{-s} \right)^{\frac{1}{2}}. \end{aligned}$$

Set  $p \rightarrow \infty$ , it follows that

$$\begin{aligned} \sum_{j=1}^{\infty} |\hat{f}_{\lambda_j}| &\leq \left( \sum_{j=1}^{\infty} |\hat{f}_{\lambda_j}|^2 (1 + |\lambda_j|^2)^s \right)^{\frac{1}{2}} \cdot \left( \sum_{j=1}^{\infty} (1 + |\lambda_j|^2)^{-s} \right)^{\frac{1}{2}} \\ &= \|f\|_{H_{QP}^s(\mathbb{R}^d)} \cdot \left( \sum_{j=1}^{\infty} (1 + |\lambda_j|^2)^{-s} \right)^{\frac{1}{2}}. \end{aligned}$$

When  $s > d/2$ , the series  $\sum_{j=1}^{\infty} (1 + |\lambda_j|^2)^{-s}$  converges. For  $f \in H_{QP}^s(\mathbb{R}^d)$ , then  $f \in L_{QP}^1(\mathbb{R}^d)$  and the Bohr-Fourier series of  $f$  is absolutely convergence. Then it converges uniformly to  $f$ . Consequently,

$$\|f\|_{L_{QP}^\infty(\mathbb{R}^d)} \leq \sum_{j=1}^{\infty} |\hat{f}_{\lambda_j}| \leq C \|f\|_{H_{QP}^s(\mathbb{R}^d)},$$

where  $C$  is a constant. Similar to the proof of Theorem 3.2, this theorem is proved.  $\square$

The error analysis of QSM without the help of parent functions is given below, see [28] for details.

**Theorem A.2** ([28]). *Suppose that  $f \in H_{QP}^\alpha(\mathbb{R}^d)$  and the nonzero minimum singular value  $\sigma_{\min}(\mathbf{P})$  of the projection matrix  $\mathbf{P}$  satisfies  $\sigma_{\min}(\mathbf{P}) > \theta > 0$ . Then, there exists a constant  $C(\theta)$ , independent of  $f$  and  $N$ , such that*

$$\|\mathcal{P}_N f - f\|_{L_{QP}^2(\mathbb{R}^d)} \leq C(\theta) N^{-\alpha} |f|_\alpha.$$

Jahnke *et al.* have proved the convergence analysis by applying OS2 method in time and the Fourier pseudo-spectral method in space to solve the Schrödinger equation with periodic potentials [2]. Therefore, based on Theorems A.1 and A.2, similar to the analysis in [2], we can obtain the error analysis of QSM-OS2.

**Theorem A.3.** *Let  $u(\cdot, t_m)$  and  $u_N^m$  be the solutions of problems (6) and (15) at  $t_m$ , respectively. Then under the conditions*

- (i) *The potential  $v$  is a  $C^1$ -smooth function and  $\|v\|_{\mathcal{X}_\alpha} \leq C$ ,  $\alpha \geq s/2 > d/4$ ;*
  - (ii) *The quasiperiodic function  $u^j \in H_{QP}^\alpha(\mathbb{R}^d)$ ,  $0 \leq j \leq m$ ;*
- the global error bound of QSM-OS2 (15) is*

$$\|u_N^m - u(\cdot, t_m)\|_{L_{QP}^2(\mathbb{R}^d)} \leq C(\tau^2 + N^{-\alpha}).$$

*The constant  $C > 0$  depends on  $C_V$ ,  $\sup\{\|u(\cdot, t)\|_{L_{QP}^2(\mathbb{R}^d)} : 0 \leq t \leq T\}$  and  $\max\{|u^j|_\alpha : 0 \leq j \leq m\}$ .*

## References

- [1] P. Dirac, The principles of quantum mechanics, Oxford University Press, 1958.
- [2] T. Jahnke and C. Lubich, Error bounds for exponential operator splittings, BIT Numerical Mathematics, 40(4): 735-744, 2000.

- [3] S. Jitomirskaya, Metal-insulator transition for the almost Mathieu operator, *Ann. Math.*, 150: 1159-1175, 1999.
- [4] L. Nixon and D. Papaconstantopoulos, Electronic structure and superconductivity of europium, *Physica C: Superconductivity and its Applications*, 47: 17-18, 2010.
- [5] L. Zhou and J. Carbotte, Particle-hole asymmetry on Hall conductivity of a topological insulator, *Phys. Rev. B*, 89(5): 085413, 2014.
- [6] P. Wang, Y. Zheng, X. Chen, C. Huang, Y. Kartashov, L. Torner, V. Konotop and F. Ye, Localization and delocalization of light in photonic Moiré lattices, *Nature*, 577: 42-46, 2020.
- [7] M. Kohmoto, Metal-Insulator transition and scaling for incommensurate systems, *Phys. Rev. Lett.*, 51(13): 1198-1201, 1983.
- [8] Y. Lahini, R. Pugatch, F. Pozzi, M. Sorel, R. Morandotti, N. Davidson and Y. Silberberg, Observation of a localization transition in quasiperiodic photonic lattices, *Phys. Rev. Lett.*, 103: 013901, 2009.
- [9] Y. Cao, V. Fatemi, S. Fang, K. Watanabe, T. Taniguchi, E. Kaxiras and P. Jarillo-Herrero, Unconventional super-conductivity in magic-angle graphene superlattices, *Nature*, 43: 556, 2018.
- [10] R. Rammal, T. Lubensky and G. Toulouse, Superconducting diamagnetism near the percolation threshold, *Journal De Physique Lettres*, 44: 65-71, 1983.
- [11] R. Merlin, K. Bajema, Roy Clarke, F. Juang and P. Bhattacharya, Quasiperiodic GaAs-AlAs Heterostructures, *Phys. Rev. Lett.*, 55: 1768, 1985.
- [12] S. Kuksin and J. Pöschel, Invariant Cantor manifolds of quasiperiodic oscillations for a nonlinear Schrödinger equation, *Ann. Math.*, 143: 149-179, 1996.
- [13] S. Kuksin, Hamiltonian perturbations of infinite-dimensional linear systems with an imaginary spectrum, *Funct. Anal. Appl.*, 21: 192-205, 1987.
- [14] J. Bourgain, Construction of quasi-periodic solutions for Hamiltonian perturbations of linear equations and applications to nonlinear PDE, *Internat. Math. Res. Notices*, 475-497, 1994.
- [15] J. Bourgain, Quasi-periodic solutions of Hamiltonian perturbations of 2D linear Schrödinger equations, *Ann. Math.*, 148: 363-439, 1998.
- [16] H. Cong, Y. Shi and W. Wang, Long-time Anderson localization for the nonlinear quasi-periodic Schrödinger equation on  $\mathbb{Z}^d$ , arXiv:2309.15706.
- [17] M. Berti and P. Bolle, Sobolev quasi-periodic solutions of multidimensional wave equations with a multiplicative potential, *Nonlinearity*, 25: 257, 2012.



- [18] M. Berti and P. Bolle, Quasi-periodic solutions with Sobolev regularity of NLS on  $\mathbb{T}^d$  with a multiplicative potential, *J. Eur. Math. Soc.*, 15: 22, 2013.
- [19] W. Wang, Space quasi-periodic standing waves for nonlinear Schrödinger equations, *Commun. Math. Phys.*, 378(2): 783-806, 2020.
- [20] W. Wang, Infinite energy quasi-periodic solutions to nonlinear Schrödinger equations on  $\mathbb{R}$ , *Int. Math. Res. Notices*, rnab327, 2022.
- [21] A. Avila, On the spectrum and Lyapunov exponent of limit periodic Schrödinger operators, *Commun. Math. Phys.*, 288: 907-918, 2009.
- [22] C. Marx and S. Jitomirskaya, Dynamics and spectral theory of quasi-periodic Schrödinger-type operators, *Ergod. Theor. Dyn. Syst.*, 37(8): 2353-2393, 2017.
- [23] S. Jitomirskaya and C. Marx, Analytic quasi-periodic Schrödinger operators and rational frequency approximants, *Geom. Funct. Anal.*, 22: 1407-1443, 2012.
- [24] D. Damanik, M. Goldstein and M. Lukic, The isospectral torus of quasi-periodic Schrödinger operators via periodic approximations, *Invent. Math.*, 207: 895-980, 2014.
- [25] K. Jiang, S. Li and P. Zhang, On the approximation of quasiperiodic functions with Diophantine frequencies by periodic functions, arXiv: 2304.04334.
- [26] K. Jiang and P. Zhang, Numerical methods for quasicrystals, *J. Comput. Phys.*, 256: 428-440, 2014.
- [27] K. Jiang and P. Zhang, Numerical mathematics of quasicrystals. *Proc. Int. Cong. of Math.*, 3, 3575-3594, 2018.
- [28] K. Jiang, S. Li and P. Zhang, Numerical methods and analysis of computing quasiperiodic systems, *SIAM J. Numer. Anal.*, in press (also see arXiv: 2210.04384).
- [29] Z. Gao, Z. Xu, Z. Yang and F. Ye, Pythagoras superposition principle for localized eigenstates of two-dimensional Moiré lattices, *Phys. Rev. A*, 108(8): 013513, 2023.
- [30] K. Jiang, J. Tong, P. Zhang and A.-C. Shi, Stability of two-dimensional soft quasicrystals, *Phys. Rev. E*, 92: 042159, 2015.
- [31] D. Cao, J. Shen and J. Xu, Computing interface with quasiperiodicity, *J. Comput. Phys.*, 424: 109863, 2021.
- [32] X. Li and K. Jiang, Numerical simulation for quasiperiodic quantum dynamical systems (in Chinese), *Journal on Numerical Methods and Computer Applications*, 42(1): 3-17, 2021.

- [33] K. Jiang, W. Si and J. Xu, Tilt grain boundaries of hexagonal structures: a spectral viewpoint, *SIAM J. Appl. Math.*, 82: 1267-1286, 2022.
- [34] C. Wang, F. Liu and H. Huang, Effective model for fractional topological corner modes in quasicrystals, *Phys. Rev. Lett.*, 129: 056403, 2022.
- [35] G. Strang, On the construction and comparison of difference schemes, *SIAM J. Numer. Anal.*, 5: 506-517, 1968.
- [36] C. Corduneanu, Almost periodic function, Second Edition, Chelsea, New York, 1989.
- [37] R. Iannacci, A. Bersani, G. Dell'Acqua and P. Santucci, Embedding theorems for Sobolev-Besicovitch spaces of almost periodic functions, *Zeitschrift Fur Analysis Und Ihre Anwendungen*, 17: 443-457, 1998.
- [38] M. Stone, Linear transformations in Hilbert space: III. Operational methods and group theory, *Proc. Natl. Acad. Sci. USA*, 16(2): 172-175, 1930.
- [39] M. Frigo and S. Johnson, The design and implementation of FFTW3, *Proc. IEEE*, 93: 216-231, 2005.